Density dependence of dielectronic recombination in selenium

Peter L. Hagelstein and Mordecai D. Rosen
Physics Department, Lawrence Livermore National Laboratory, Livermore, California 94550

Verne L. Jacobs
E. O. Hulburt Center for Space Research, Naval Research Laboratory, Washington, D.C. 20375

(Received 31 March 1986)

Dielectronic recombination has been found to be the dominant recombination process in the determination of the ionization balance of selenium near the Ne-like sequence under conditions relevant to the exploding-foil EUV laser plasmas. The dielectronic recombination process tends to populate excited levels, and these levels in turn are more susceptible to subsequent excitation and ionization than are the ground-state ions. If one defines an effective recombination rate which includes, in addition to the primary recombination, the subsequent excitation and ionization of the additional excited-state population due to the primary recombination, then this effective recombination rate can be density-sensitive at relatively low electron density. We present results for this effective dielectronic recombination rate at an electron density of 3×10^{20} electrons/cm^3 for recombination from Ne-like to Na-like selenium and from F-like to Ne-like selenium. In the former case, the effective recombination rate coefficient is found to be 1.8×10^{-11} cm^3/sec at 1.0 keV, which is to be compared with the zero-density value of 2.8×10^{-11} cm^3/sec. In the latter case (F-like to Ne-like), the effective recombination rate coefficient is found to be 1.3×10^{-11} cm^3/sec, which is substantially reduced from the zero-density result of 3.3×10^{-11} cm^3/sec. We have examined the effects of dielectronic recombination on the laser gain of the dominant Ne-like $3p$-$3s$ transitions and have compared our results with those presented by Whitten *et al.* [Phys. Rev. A 33, 2171 (1986)]. The results obtained for the gain of the $J=2$ transitions at 206.9 and 209.8 Å disagree by a factor of 2, and the calculated F-like to Ne-like isoelectronic sequence ratio differs by a factor of 4. These discrepancies are investigated and are found to be due to three factors: inclusion of post-recombination collision effects, inclusion of Rydberg levels, and choice of line shape.

I. INTRODUCTION

Dielectronic recombination can play an important role in the determination of the ionization balance of a non—local-thermodynamic-equilibrium (LTE) plasma[1] and in the formation of excited-state population.[2,3] Dielectronic recombination is a multistep process in which an electron undergoes radiationless capture into an autoionizing doubly excited state and subsequent stabilization by radiative decay or by some other atomic process. The final product of this stabilization may be a ground state or a singly excited state of the recombined ion, and such a state may undergo further excitation or ionization subsequently.[4,5] Although these subsequent processes are independent of the primary dielectronic recombination process, they can be treated as producing a reduction of the dielectronic recombination rate.

Consider an example where the radiationless capture together with the stabilization leads predominantly to singly excited states which are of moderate excitation. Dielectronic recombination in low-Z systems tend to occur predominantly through such processes. The recombination process then provides a source for the creation of such moderately excited states, and the populations of such levels will be enhanced above their values in the absence of dielectronic recombination. These moderately excited states will be more susceptible to subsequent excitation and ionization than will be the ground state of the same ion, and their presence will enhance the total ionization rate of the ionization stage in proportion to the dielectronic recombination rate.

One might be tempted to model the post-recombination effects through a reduction of the zero-density dielectronic recombination rate. Whether this rate is or is not viewed as reduced depends on how the dielectronic recombination process is defined. One definition might be that the dielectronic recombination process includes all steps up to the stabilization into singly excited levels. All subsequent collisional and radiative processes affecting the populations of the singly excited states are then distinct processes which are to be included separately. Another definition of the dielectronic recombination process might be that only primary dielectronic recombination which is followed by kinetics processes that ultimately produce ground-state ions is to be counted as part of the dielectronic recombination process.

The first view would be most suitable for inclusion in a kinetics model where the singly excited states are treated either in a detailed manner or by some averaged (Rydberg) method. In such a case, one requires the detailed recombination information specific to every level accounted for in the kinetics model, and the net ionization and recombination rates between ionization stages will be incorporated self-consistently. The second view would be more

useful in a kinetics model where only ground states are included, or in a detailed model where the dielectronic recombination rates are applied only between ground states.

In this paper we present some new results for dielectronic recombination from F-like to Ne-like selenium. A recent paper of Apruzese *et al.*[6] has presented a low value (3.4×10^{-12} cm^3/sec) for the corresponding recombination rate coefficient, and we find that it disagrees with the present results in both the collisional and collisionless limits. Because the interpretations presented by Apruzese *et al.*[6] follow in part from the choice of the dielectronic recombination coefficient, this issue is relevant to the theoretical explanation of the observed EUV amplification. This has been discussed by Whitten *et al.*,[2] and the dielectronic recombination rate coefficient given in their work [$(2.8-3.5)\times10^{-11}$ cm^3/sec], which is a zero-density result, might be recommended with caution for use in plasmas of such high-electron density (5×10^{20} electrons/cm^3). The effective ground-state to ground-state dielectronic recombination coefficient, which is more appropriate for ionization balance calculations, can be obtained using the method described in the present work. In Sec. V, we treat these plasma conditions and find an effective recombination rate coefficient of 1.16×10^{-11} cm^3/sec.

In the work by Whitten *et al.*,[2] an analysis of the effects of dielectronic recombination on excited-state populations and gain in Ne-like selenium has been presented, and substantial effects due to the recombination into excited states have been reported. The present results are not in good agreement with those of Whitten *et al.*,[2] and the disagreement has included a factor of 2 in gain on the $J=2$ lines at 206.9 and 209.8 Å and a factor of 4 in the F-like to Ne-like ion population ratio. These discrepancies have been a source of concern, and in this work we attempt to resolve these issues. Through a number of comparisons between the results of the two models on simple benchmark steady-state problems, we find that only a relatively small difference can be attributed to the atomic physics data (mostly collisional cross sections) included between the 37 levels of the Ne-like L- and M-shell states. However, three main factors can account for most of the remaining discrepancies: inclusion of the effects of post-recombination kinetics, inclusion of Rydberg levels, and choice of line shape.

II. DETAILED KINETICS MODELING IN SELENIUM

The model described here is an improved version of the one used in the EUV laser design calculations presented by Rosen *et al.*,[7] who give a brief description of this model. The model contains 494 levels altogether, and it includes detailed excited-state level structure for the Na-, Ne, and F-like isoelectronic sequences. Most of the atomic physics data used in the model was generated using the fully relativistic multiconfigurational atomic physics code of Hagelstein and Jung[8] (the YODA code). The electron collisional excitation cross sections for the neonlike sequence are given by Hagelstein and Jung,[9] and the F-like cross sections are tabulated by Hagelstein.[10] Detailed recombination rate coefficients obtained from the YODA relativistic model are included. These coefficients have been described elsewhere for the Ne-like sequence[11] and for the F-like ion.[3,12]

The sodiumlike level structure includes the 12 M-shell and N-shell states in detail (with resolved fine structure) and Rydberg states from $n=5$ to $n=10$. The Ne-like model includes the L-, M-, and N-shell states in detail (89 levels) and an additional set of 3 Rydberg series (from $n=5$ to $n=10$) leading to the three F-like ground states. The F-like model contains the 113 L- and M-shell states in detail and 3 Rydberg series leading to the low-lying O-like configurations $2s^22p^4$, $2s2p^5$, and $2p^6$.

The Mg-like through Cl-like isoelectronic sequences are described using hydrogenic models originally generated by the XATOM code of Morgan *et al.*[13] and substantially revised. The He-like through O-like sequences are treated in an approximation which is somewhat more sophisticated than hydrogenic (the "Hartree-Fock" model of XATOM, with subsequent improvements). In all sequences, consistent dielectronic recombination models based on the $\bar{f}$ and $\bar{\lambda}$ model of Hagelstein[3,12] have been included. We have used the non-LTE code XRASER (Ref. 14) to construct and solve the rate equations for population kinetics calculations utilized in Sec. III.

Our procedure for determining an effective recombination rate which includes the effects of post-recombination collision processes may be described simply. We first carry out a non-LTE calculation using the full kinetics model and note the sequence populations and $\bar{Z}$. We then remove all detailed "zero-density" dielectronic recombination rates from the model, and in their place we introduce a single ground-state to ground-state recombination rate coefficient. The steady-state calculation is then repeated with different values of the effective recombination rate coefficient until the sequence populations which are obtained from our initial full calculation are reproduced. For the determination of the effective rate coefficients for Ne-like recombination, we were able to obtain good agreement on both sequence populations and $\bar{Z}$. In the calculations of the F-like recombination coefficients, we were not able to obtain precise agreement between sequence populations, and our results are based on matching $\bar{Z}$.

III. RECOMBINATION FROM Ne-LIKE SELENIUM

There are several ways in which density effects may modify the effective dielectronic recombination rate, and the post-recombination collisional effects tend to be the most important at moderate densities (near 10^{20} electrons/cm^3) for Ne-like selenium. As the density increases, electron collisional redistribution of the doubly excited level populations can occur. We have previously investigated the effects of dipole-allowed collisional transitions within the $3l3l'$ doubly excited manifold of the sodiumlike ion,[11] and have found that these effects become significant for densities above 10^{21} electrons/cm^3, where an increase in the primary dielectronic recombination rate occurs.

Doubly excited states of the form $2p^5 3lnl'$ are primarily responsible for producing the moderately excited $2p^6 nl'$ Na-like states (following 3-2 stabilizing radiative decay) under conditions of interest here. The effects of dipole-allowed collisional transitions on the excited nl' electron (for n greater than 3) of the doubly excited state will occur at a lower electron density than for the $3l$ electron, and therefore one might expect to see increases in the primary dielectronic recombination rate at substantially lower densities.

This argument is misleading for the following reason: in the $3l3l'$ case, collisional mixing enhanced the recombination rate because new routes were opened by which a $3l$ electron could undergo a radiative 3-2 decay. The dominant contributions arise from the states which are stabilized by the fast $3d$-$2p$ radiative transitions, with decay rates near 10^{14} sec^{-1}. The $3lnl'$ states are stabilized principally by 3-2 decay as well, and it is the $3l$ electron which must undergo collisional transitions to cause any significant enhancement of the primary dielectronic recombination rate. The reason for this is that the radiative stabilization rate is faster than the autoionization rate, and therefore most of the population which is captured into a doubly excited $3lnl'$ state of moderate n is stabilized, independent of n and l'. Consequently the l-changing collisional mixing of the excited nl' electron, which may occur at moderate electron density, should have only a second-order effect on the primary dielectronic recombination rate.

Our approximation is then that the primary radiationless capture and stabilization remains unaffected by electron collisions or other density effects; that the singly excited states which are the final products of the stabilization are allowed to undergo subsequent excitation and ionization; and that all other processes are treated with the relatively complete kinetics models described briefly above.

The effects of post-recombination collisional processes on the effective dielectronic recombination rate coefficient can be seen from an examination of Fig. 1, in which both the zero-density and a finite density ($N_e = 3\times10^{20}$ electrons/cm^3) dielectronic recombination rate coefficients from the Ne-like ground state are plotted as functions of electron temperature. At 1 keV, the effective recombination rate coefficient is about 61% of the value at low density. The reduction in the effective recombination rate coefficient is less at low temperature, where the recombination is dominated by capture into the $2p^5 3l3l'$ states, which undergo radiative stabilization to the low-lying sodiumlike M-shell states. The effective dielectronic recombination rate coefficient has been defined to be a ground-state to ground-state-rate coefficient, and therefore the two rate coefficients become equal at low temperature.

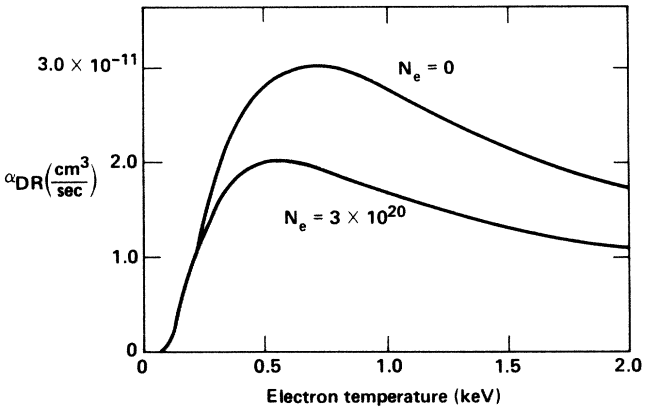

FIG. 1. Zero-density dielectronic recombination rate coefficient and effective dielectronic recombination coefficient at $N_e = 3\times10^{20}$ electrons/cm^3 for recombination from Ne-like selenium to Na-like selenium, as functions of electron temperature.

IV. RECOMBINATION FROM F-LIKE SELENIUM

We have carried out an analysis similar to that presented in Sec. III for recombination from F-like selenium. The low-density results were given previously.[3] In this case there are three low-lying F-like states, consisting of the $^2P_{3/2}$, $^2P_{1/2}$, and $^2S_{1/2}$, and each state has a different total recombination rate coefficient. We have chosen to introduce a single effective average recombination rate coefficient which connects each of the three states with the Ne-like ground state and which has the same numerical value for each of the three F-like states. It would be possible to revise the procedure under the assumption of a separate effective recombination rate coefficient for the three low-lying F-like states. We have not done this here, as the calculation would involve substantial effort and would add little to the basic physics under discussion in this work.

The results are shown in Fig. 2 for the same plasma electron density considered above (3×10^{20} electrons/cm^3).

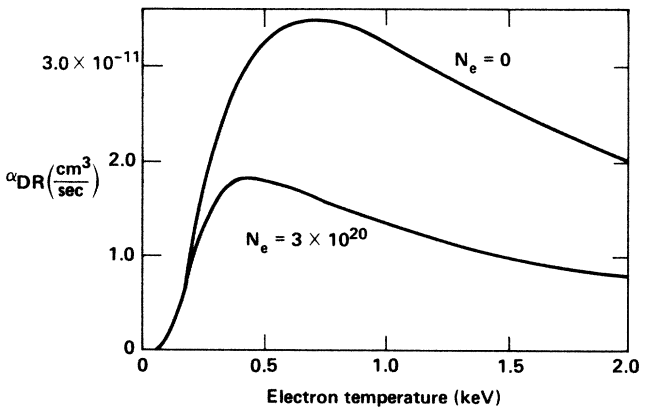

FIG. 2. Zero-density dielectronic recombination rate coefficient and effective dielectronic recombination coefficient at $N_e = 3\times10^{20}$ electrons/cm^3 for recombination from F-like selenium to Ne-like selenium, as functions of electron temperature. The zero-density result is for recombination from the F-like ground state $2s^2 2p^5\,^2P_{3/2}$, and the finite density result is computed assuming that the three low-lying F-like states have the same effective recombination rate coefficients. No recombination resulting from the 2-2 inverse Coster-Kronig process is included in either result.

In this case we obtain a larger zero-density rate coefficient than in the Ne-like case (a peak rate coefficient of 3.5×10^{-11} cm^3/sec for the F-like $^2P_{3/2}$, which is to be compared with the value 3.0×10^{-11} cm/sec for the Ne-like $^1S_0$ state), and a smaller effective recombination rate coefficient than before (peak values of 1.8×10^{-11} cm^3/sec for the F-like ion, which is to be compared with the peak value of 2.0×10^{-11} cm^3/sec for the Ne-like ion). The density effects are more pronounced in the recombination from the F-like sequence. At 1 keV, the effective recombination rate coefficient is calculated to be only 41% of the zero-density result.

It might be surprising that the density effects are stronger for F to Ne-like recombination than for Ne to Na-like recombination. The primary capture and stabilization is similar for the two cases, and the zero-density recombination into the singly excited M-shell, N-shell, and Rydberg levels is not particularly different between the two cases. As a result, it is not obvious that there should be differences in the density dependence of the effective recombination rate coefficient. The explanation of these differences appears to involve the details of the level structure of the singly excited states of the Na- and Ne-like ions. Recombination from F- to Ne-like ions produces singly excited M-shell states, many of which are metastable (that is, do not immediately decay to the $2s^22p^6\,^1S_0$ ground state). In addition, much of the recombination into the more highly excited levels ultimately produces M-shell metastable population. These metastables are susceptible to collisional excitation and eventual ionization, and it is these states which lead to the more pronounced density dependence of the effective dielectronic recombination rate coefficient for the F-like ion.

The results of this section and of Sec. III should be compared with the recombination rate coefficient quoted by Apruzese *et al.*,[6] which is 3.4×10^{-12} cm^3/sec. One finds that the recombination rate coefficient quoted in their work is lower by a factor of about 5 in comparison with the density-reduced values quoted here and is roughly a factor of 10 less than our low-density limit.

In the paper of Whitten *et al.*,[2] an explanation is given for the lower result quoted by Apruzese *et al.*,[6] and it may be useful to attempt further clarification here. The procedure of extrapolating threshold excitation cross sections to obtain Auger rates and dielectronic recombination rate coefficients is well known and, judging from the detailed comparisons by Hagelstein,[12] should lead to relatively accurate results in selenium. Errors as large as 50% may be expected under such conditions, but not errors of a factor of 10.[15] The discrepancy is most probably attributable to a different approximation, in which the $3l$-$3l'$ Coster-Kronig autoionization process, which may compete with the 3-2 radiative stabilization, was assumed to be energetically permissable for all doubly excited states, regardless of the value of principal quantum number n.

At low Z, the Coster-Kronig process plays an important role in reducing the recombination rate, because the high Rydberg $3lnl'$ states which play the dominant role can decay via this autoionization process. Adoption of a model based on the assumption that the Coster-Kronig decay is allowed for all values of n is expected to give questionable results at moderately high Z,[16] where such processes are energetically forbidden. The validity of this approximation has been discussed in a recent investigation.[16] We note that the present results are in good agreement with the rate coefficients used by Rosen *et al.*,[7] thus bringing into question the main results of Apruzese *et al.*[6]

V. RECOMBINATION PUMPING OF EXCITED STATES

The dielectronic recombination from F-like selenium into the singly excited states of Ne-like selenium alters the singly excited state populations, and the theoretical predictions of laser gain of 206 and 209-Å transitions are sensitive to the inclusion of this process. Our results indicate that theoretical models which include this process produce better agreement with the experimental results for exploding-foil targets for both the 206- and 209-Å strong laser transitions which have $J=2$ upper laser states. However, disagreement remains for the value of gain of the 182-Å laser transition from the $J=0$ upper state.

employed by Whitten *et al.*,[2] and we have compared our results with theirs. Although it was known that the results obtained from the simple modeling were not in good agreement with the results of the design model simulations discussed above, until now little effort has been invested in identifying the differences. The principal differences include a factor of 4 in Ne- to F-like ratio and factor of 2 in calculated laser gain for the $J=2$ lines. In addition, the model of Whitten *et al.*[2] did not take into account the effects of post-recombination collisional processes discussed here, because Rydberg levels above $n=4$ were not included. What differences this made in the calculated results for gain are of interest, especially given the relatively large reductions in effective recombination coefficients as discussed in Sec. IV.

These issues can be explored by considering the results tabulated in Table I, where a number of models of varying complexity have been compared on the steady-state problem of Whitten *et al.*[2] The plasma conditions are assumed in all cases to be those of Whitten *et al.*,[2] wherein the electron density is taken to be 5×10^{20} electrons/cm^3, the electron temperature is 1.0 keV, and the ion temperature is 0.4 keV. In the first four models, only the Ne-like isoelectronic sequence is included in the calculation, and the ion density of the sequence is 5×10^{18} ions/cm^3. In models 5—12, both the Ne- and F-like ionization stages are present, and in both cases the Ne-like ion density is fixed at 5×10^{18} ions/cm^3. The final two models (13 and 14) were applied in the presence of many ionization stages, and the overall ionization balance was determined self-consistently. In this case the Ne-like ion density was somewhat lower (3.23×10^{18} ions/cm^3). Consequently models 1—12 represent basically different approximations to the same test problem, and models 13 and 14 represent an approximation to the actual ion kinetics including the effects of ionization balance. These models differ from those used in the full design simulations only in the nonessential restriction to a steady-state condition.

TABLE I. Comparison of gains of the $3p$-$3s$ main laser lines in Ne-like selenium. All calculations assume an electron density of 5×10^{20} electrons/cm^3, an electron temperature of 1.0 keV, and an ion temperature of 0.4 keV. Models 1 to 12 are defined to have the same number of Ne-like ions (5×10^{18} cm^{-3}), while in models 13 and 14 the ionization balance was established self-consistently with the above electron density under the assumption that only selenium is present. For models 13 and 14, the Ne-like density is 3.23×10^{18} cm^{-3}. The models of Whitten *et al.* are published in Ref. 2.

	Model	Ne-like $n=4$ levels	F-like levels	Rydberg levels	Dielectronic recombination	Line shape	Gain 182.4 Å	Gain 209.8 Å	Gain 206.9 Å	N_F/N_{Ne}
1	Whitten (37)	No	No	No	No	Doppler	14.3	11.4	9.7	0
2	XRASER (37)	No	No	No	No	Doppler	17.4	10.1	11.9	0
3	Whitten (89)	Yes	No	No	No	Doppler	13.4	13.0	11.5	0
4	XRASER (89)	Yes	No	No	No	Doppler	16.1	11.7	13.9	0
5	Whitten (89/3)	Yes	Yes	No	Yes	Doppler	13.0	15.3	13.6	0.6
6	XRASER (89/3)	Yes	Yes	No	Yes	Doppler	15.4	14.1	16.1	0.58
7	XRASER (89/3)	Yes	Yes	No	Yes	Voigt	11.7	10.4	11.2	0.58
8	Whitten (89/3)	Yes	Yes	No	Yes	Doppler	11.9	21.7	19.4	2.62
9	XRASER (104/189)	Yes	Yes	Yes	Yes[a]	Doppler	16.4	5.6	6.0	2.62
10	XRASER (104/189)	Yes	Yes	Yes	Yes	Doppler	14.5	14.5	14.2	2.62
11	XRASER (104/189)	Yes	Yes	Yes	Yes[a]	Voigt	12.3	4.1	4.1	2.62
12	XRASER (104/189)	Yes	Yes	Yes	Yes	Voigt	11.0	10.6	9.8	2.62
13	XRASER (Full)	Yes	Yes	Yes	Yes[a]	Voigt	8.0	2.6	2.7	2.62
14	XRASER (Full)	Yes	Yes	Yes	Yes	Voigt	7.1	6.8	6.3	2.62

[a]In models 9, 11 and 13, an effective ground-state to ground-state recombination rate between the F- and Ne-like sequence was used in place of the detailed recombination model and adjusted to obtain an ionization balance in agreement with the detailed model. In these models, dielectronic recombination into the excited-state populations is not included.

In all calculations using the XRASER design model described here, either the actual atomic data was extracted from the full kinetics model (models 2, 4, 6, and 7), or else the model was carried out with either a reduced set of ionization stages (models 9—12) or a full set of ionization stages (models 13 and 14).

The basic Ne-like L-shell and M-shell models are assessed in the comparison of results of models 1 and 2. The laser gain of the $J=0$ transition is higher in the present results due to a larger monopole $2p$-$3p$ collisional excitation cross section, which gives rise to differences as large as 20%. In a 37-level model, indirect excitation is responsible for the gain on the $J=2$ transitions, and similar differences are apparent. The model of Ref. 2 was constructed using an incomplete set of cross sections computed using the University College London code SUPERSTRUCTURE,[17] and the present results are modeled using a full set of cross sections obtained by Hagelstein and Jung.[9] The agreement between the results obtained from these models is at the 20% level, and these differences may be attributed primarily to differences in the included electron collisional cross sections. Agreement to 20% is reasonable, although further work on the physics of the simple 37-level model may be worthwhile.

The more complex 89-level models are compared in models 3 and 4. Relative to the 37-level models, both the results of Whitten *et al.*[2] and the present results show a similar decrease in the gain of the 182-Å line and an increase in the gain of the 206- and 209-Å lines. When the three lowest F-like levels are added to the 89-level Ne-like model (with no Rydberg levels), the effects of recombination (dielectronic and otherwise) can be investigated (models 5 and 6). Nearly equal increases in laser gain for the $J=2$ lines are again obtained from the two models. In fact, if the gain obtained for the 209-Å line from model 6 is increased by 1.3 cm^{-1} due to differences in the 37-level model atomic physics (models 1 and 2), the resulting adjusted gain of 15.4 cm^{-1} is in excellent agreement with the result of 15.3 cm^{-1} predicted by model 5.

A Doppler profile was adopted for describing the laser line shape in the paper of Whitten *et al.*[2] Our calculations allow for a Voigt profile, with the Lorentz contribution obtained by summing all outgoing kinetics rates from both the upper and lower levels of a laser transition.[7,10,14] The gain is sensitive to the line profile for all three transitions, as can be seen from a comparison of the results obtained from models 6 and 7, which are identical except for the choice of profile. The reduction of gain due to the use of a more realistic line profile is between 25% and 30%.

We next consider the role of the Rydberg levels corresponding to $n=5$ through $n=10$, whose effects may be seen from inspection of the results from models 8 through 10 in Table I. The inclusion of these Rydberg levels in the model tends to substantially alter the ionization balance, and in the XRASER models one finds a ratio of F to Ne-like population of 2.62. This value is in agreement with the results calculated using the full XRASER model. The resulting increase in F- to Ne-like ratio may be understood by noting that stepwise excitation up through the Rydberg levels, followed by ionization from these levels, provides

the dominant ionization mechanism for ground-state Ne-like ions.

Results are presented by Whitten *et al.*[2] for arbitrary values of the F- to Ne-like ion ratio, and we may compare our results with theirs. For model 8, we have taken the values of gain from Fig. 1 of their paper, and we have tabulated the results for our value of F- to Ne-like ion ratio.

Model 9 is a detailed two-sequence model with the dielectronic recombination processes accounted for by an effective ground-state to ground-state rate coefficient. The zero-density recombination rate coefficient from the $^2P_{3/2}$ is 3.27×10^{-11} cm^3/sec. This may be compared with the $3l3l'$ and $3l4l'$ results of Chen, tabulated in Ref. 2, which is equal to 2.22×10^{-11} cm^3/sec at 1.0 keV. This result is also within the range of the estimated total rate coefficient of $(2.8-3.5)\times10^{-11}$ cm^3/sec quoted in Whitten *et al.*[2] The effective ground-state to ground-state recombination rate coefficient required to reproduce the ionization balance obtained from full design model is 1.16×10^{-11} cm^3/sec. This model gives an ionization balance between the F- and Ne-like sequences which is consistent with that of the full model, and it is defined to have a Ne-like ion population of 5×10^{18} ions/cm^3. In addition, it excludes the effect of dielectronic recombination on the excited states.

Model 10 is identical to model 9 aside from description of dielectronic recombination. Where model 9 included the effects of dielectronic recombination as an effective ground-state to ground-state rate, model 10 includes the detailed dielectronic recombination model in which the recombination populates singly excited Ne-like states. A comparison of models 9 and 10 reveals the effects of dielectronic recombination on the Ne-likely singly excited level populations and on the laser gain, with the assumption of a Doppler profile. A comparison of models 8 and 10 indicates how much of a reduction in gain might be expected to result from the inclusion of the Rydberg levels in the analysis of Whitten *et al.*[2] The reduction in gain is due primarily to a reduction of the effective dielectronic recombination rate due to post-recombination kinetics effects.

Models 11 and 12 are identical with models 9 and 10 aside from the choice of line profile; the two earlier models include Doppler profiles and the later models, 11 and 12, are based on a Voigt profile for the line shape. The results of model 12 should be considered to be the most accurate for this simple representative problem, because Rydberg levels, dielectronic recombination, a realistic line shape, and improved ionization balance are included.

It is of interest to consider the full calculation of the kinetics and gain under the plasma conditions of an electron temperature of 1.0 keV and an electron density of 5.0×10^{20} electrons/cm^3. This problem would be substantially more difficult in that the ionization balance problem must be dealt with in its fullness in order to obtain an accurate result. In models 13 and 14, we present results for this modified problem. Model 13 includes the extensive multisequence level structure with the detailed description of dielectronic recombination from F-like to Ne-like selenium replaced by an effective ground-state to ground-state rate coefficients as above. Model 14 is the full design model including the detailed description of dielectronic recombination.

Under these conditions, the plasma is predicted to be ionized well past the Ne-like sequence, and consequently the absolute number of Ne-like ions present is computed to be 3.23×10^{18} ions/cm^3. This is less than the 5.0×10^{18} ions/cm^3 of the test problems of models 1–12, and hence the results are not directly comparable. One observes that without dielectronic recombination populating the excited levels, the $J=0$ transition has a markedly higher gain than for the $J=2$ lines. This observation is consistent with the simulation results which we routinely obtained in our design calculations from 1983 through early 1985.[7] The effects of dielectronic recombination on the singly excited state Ne-like populations increase the gains of the $J=2$ transitions to values close to that of the $J=0$ transition, although from inspection of model 14, the 182.4-Å line is seen still to have the largest gain. This result is consistent with our current time-dependent simulations.[18]

Radiation from the $J=0$ transition is observed to be amplified in the selenium lasers which have been tested this year, although the laser gain remains less than that predicted by our theoretical modeling. The gain of the $J=2$ transitions is comparable to that predicted by our design simulations.[19]

VI. SUMMARY AND CONCLUSIONS

We have investigated the effects of post-recombination kinetics processes on dielectronic recombination from Ne- and F-like selenium. The extensive multisequence non-LTE kinetics model of selenium, which has been developed during the last several years, has been revised to incorporate a detailed description of dielectronic recombination which explicitly allows for recombination into excited states, and which takes into account the post-recombination kinetics processes. At low density, this dielectronic recombination model reproduces the known zero-density dielectronic recombination coefficients reported previously.[2,3] At moderate electron densities such that the effects of l-changing collisions on the populations of the doubly excited states do not affect the primary recombination, this model self-consistently describes the reduction of the dielectronic recombination coefficient due to post-recombination kinetics processes.

The dielectronic recombination rate coefficient from Ne- to Na-like selenium was presented for the case of zero electron density, and an effective ground-state to ground-state recombination rate coefficient which reproduces the ionization balance for $N_e=3\times10^{20}$ electrons/cm^3 was calculated and presented (Fig. 1). The effective rate is found to be reduced to 61% of the zero-density rate at 1 keV.

The recombination rate coefficient from F- to Ne-like was presented for dielectronic recombination from the $^2P_{3/2}$ state for zero electron density, and an effective recombination rate coefficient including post-recombination kinetics at $N_e=3\times10^{20}$ electrons/cm^3 was computed and presented (Fig. 2). The effective recombination rate is found to be reduced to 41% of the zero-density result.

The effects of dielectronic recombination on the gain of the Ne-like $3p$-$3s$ laser transitions at 182.4, 206.9, and 209.8 Å were investigated and compared with the results of a simple model of Whitten *et al.*,[2] for a restricted test problem at $T_e = 1.0$ keV and $N_e = 5.0 \times 10^{20}$ electrons/cm^3. Since the present model that of Whitten *et al.*[2] contain much atomic data which comes from different sources, we compared the basic 37-level models of the Ne-like L- and M-shell levels and found agreement to within 20%.

Comparisons of models including the 89 Ne-like L-, M-, and N-shell levels, and three F-like levels showed excellent agreement, such that the differences in gain could be accounted for only by the differences between the basic 37-level models. In these comparisons, where no Rydberg states were included in either model, the ratio of F- to Ne-like populations could be reproduced by the two models to give the result of 0.6.

The inclusion of the Rydberg levels in the Ne-like sequence caused a significant shift in ionization balance, increasing the F- to Ne-like ratio to 2.6, and altered the gain by a small amount. Inclusion of a more realistic description of line shape (replacing the Doppler profile by the Voigt profile) resulted in a reduction in gain of 25—30%. The net result is a reduction by a factor of 2 from the results of Whitten *et al.*[2] (models 8 of our Table I) for the $J = 2$ lines in comparison with the present results (model 14 of Table I). These results explain most of the discrepancies between our model and that of Whitten *et al.*[2]

Note added in proof. An improved version of the design model has been developed as this work was in press, where the modifications consist of improved $\langle \sigma v \rangle$ fitting coefficients for the Ne-like and F-like sequences, and the inclusion of distorted wave $\langle \sigma v \rangle$ results for most of the Ne-like 3-4 transitions. We have recalculated model 14 of Table I, and have obtained a new result for the neonlike population (3.43×10^{18}/cm^3) and a higher result for the 209 Å gain (7.1 cm^{-1}). The gains for the 182 and 206 Å lines remained the same. The F-like to Ne-like ion ratio is now 2.66.

ACKNOWLEDGMENTS

The authors are indebted to L. Minner and R. Jung for their expertise and hard work in the development and support of the codes used in the numerical calculations presented in this work. M. Chen contributed numerous comments and suggestions from which we benefited. This work was performed under the auspices of the U.S. Department of Energy by Lawrence Livermore National Laboratory under Contract No. W-7405-Eng-48.

[1] A. Burgess and M. J. Seaton, Mon. Not. R. Astron. Soc. **127**, 355 (1964).

[2] B. L. Whitten, A. U. Hazi, M. H. Chen, and P. L. Hagelstein, Phys. Rev. A **33**, 2171 (1986).

[3] P. L. Hagelstein, Lawrence Livermore National Laboratory Report No. UCRL-93811, 1985 (unpublished).

[4] A. Burgess and H. P. Summers, Astrophys. J. **157**, 1007 (1969).

[5] V. L. Jacobs and J. Davis, Phys. Rev. A **18**, 697 (1978).

[6] J. P. Apruzese, J. Davis, M. Blaha, P. C. Kepple, and V. Jacobs, Phys. Rev. Lett. **55**, 1877 (1985).

[7] M. D. Rosen, P. L. Hagelstein, D. L. Matthews, E. M. Campbell, A. U. Hazi, B. L. Whitten, B. MacGowan, R. E. Turner, R. W. Lee, G. Charatis, Gar. E. Busch, C. L. Shepard, P. D. Rockett, and R. R. Johnson, Phys. Rev. Lett. **54**, 106 (1985).

[8] P. L. Hagelstein and R. K. Jung (unpublished). Also, presented at the 3rd International Conference/Workshop on the Radiative Properties of Hot Dense Matter, Williamsburg, Virginia, 1985 (unpublished).

[9] P. L. Hagelstein and R. K. Jung, At. Data Nucl. Data Tables (to be published).

[10] P. L. Hagelstein, Phys. Rev. A **34**, 924 (1986).

[11] S. Dalhed, J. Nilsen and P. Hagelstein, Phys. Rev. A **33**, 264 (1986).

[12] P. L. Hagelstein (unpublished).

[13] W. L. Morgan, D. R. Kim, R. K. Jung, and W. E. Alley, *Fifth Topical Conference on Atomic Processes in High Temperature Plasmas, Monterey, California, 1985* (unpublished).

[14] P. L. Hagelstein, M.I.T. Ph.D. thesis (1981). Available as Lawrence Livermore National Laboratory Report No. UCRL-53100, 1981 (unpublished).

[15] In fact, a direct calculation of the zero-density dielectronic recombination rate coefficient based on the extrapolation of threshold partial-wave collisional cross sections and which takes into account the fact that the Coster-Kronig autoionization processes from the low-lying doubly excited states are energetically forbidden, has been carried out by one of the authors (V.L.J.). The results of this new calculation are in reasonable agreement with the results of Fig. 2. In this calculation, inclusion of recombination channels involving $3d$-$2p$ and $3s$-$2p$ stabilizing radiative decays leads to a dielectronic recombination coefficient of 2.7×10^{-11} cm^3/sec at 862 eV. The value from Fig. 2 at 862 eV is 3.4×10^{-11} cm^3/sec, which is in agreement to within 25%.

[16] V. L. Jacobs, Astrophys. J. **296**, 121 (1985).

[17] W. Eissner, M. Jones, and H. Nussbaumer, Comput. Phys. Commun. **8**, 270 (1974); W. Eissner and M. J. Seaton, J. Phys. B **5**, 2187 (1972); H. E. Saraph, Comput. Phys. Commun. **1**, 232 (1970); *ibid.* **3**, 256 (1972).

[18] D. L. Rosen and P. L. Hagelstein, Proceedings of the Conference on Generation of Coherent Radiation in the Extreme Ultraviolet, Monterey, California, 1986 (unpublished).

[19] D. L. Matthews, Ref. 18.